

# Visual search in angiograms: does geometry play a role in saliency?

J.P. Rolland and C.S. Helvig

Department of Computer Science, University of North Carolina, Chapel Hill, NC 27599  
rolland@creol.ucf.edu

## ABSTRACT

Quantifying and modeling how the human eye searches medical images is important. Equally detectable lesions may not be equally salient in a visual search. This research investigates the effect of geometry on the saliency of stenoses in angiograms. A previous experiment suggested that stenoses located in areas of high curvature along vessels would be less salient.<sup>1</sup> In this paper, we measure the saliency of stenoses in two steps: first, we measure stenoses amplitude detection thresholds for stenoses at three values of curvature along vessels; second, after adjusting the degree of stenosis at these curvatures to multiples of the measured thresholds to achieve equal detectability, we measure the saliency of the stenoses in a visual search experiment. Median reaction time is used as a measure of saliency. We found that thresholds increase as curvature increases. This finding explains the decrease in saliency found in a previous investigation.<sup>1</sup> Results also show that median reaction time is constant across different curvatures for 70% and higher degrees of stenosis, indicating that saliency is independent of geometry for clinically significant angiographic lesions.

Keywords : background complexity; geometry; preattentive; saliency; shape discrimination; visual search.

## 1. INTRODUCTION

The modeling of search for relevant features in realistic backgrounds such as medical images is still in its infancy today. It is important to investigate such a model because of the significant rate of misses reported in the clinic that are still not fully understood.<sup>2</sup> Moreover, such a model will facilitate medical imaging system optimization and may provide additional guidelines for computer-assisted diagnosis.

A unified model of search in medical images requires accounting for various types of background complexities. Some models of human performance have been derived to predict detectability of lesions at unknown locations, given the detectability at known locations.<sup>3-7</sup> An important question is whether the saliency of an object in a complex background can be solely predicted from the object's detectability measured in a task where the object's location is known exactly or whether other factors such as geometry and context contribute to saliency in a more complex fashion. This research addresses the question whether geometry plays a role in finding features of interest embedded in complex geometrical backgrounds.

The challenge of assessing image quality in complex realistic backgrounds stems, in part, from the difficulty in characterizing background complexity.\* Recent advances towards the assessment of image quality in complex backgrounds are the measure of detectability of discs in mathematically defined complex backgrounds, referred to as lumpy backgrounds.<sup>8-12</sup> Those backgrounds may well simulate medical images such as mammograms, where higher lumpiness in the background may account for regions of higher density in breast tissue.<sup>13</sup> Other types of background complexities are salient background features such as bones in chest radiographs, and rich geometry such as those found in angiograms.<sup>14,15,1</sup> Most background complexities are difficult to characterize mathematically.<sup>16</sup>

We propose to quantify the detection of abnormalities in 2-D simulated angiograms because they are rich in geometry, and they can be mathematically defined and characterized.<sup>17</sup> The two basic tasks performed with angiograms are the detection of bulges (aneurysms) and narrowing (stenoses) in blood vessels and the estimation of their extents.<sup>18-20</sup> The presence of either an aneurysm or a stenosis in a blood vessel may be indicative of a vascular disease. Accurate diagnosis is essential in prevention of catastrophic vascular malfunction resulting from the rupture of an aneurysm or constricted blood flow in a major vessel.<sup>21</sup>

In a previous paper, we suggested a new methodology to quantify feature saliency in complex backgrounds.<sup>1,22</sup> We proposed a two step procedure: the first step consisted in measuring the detection thresholds of features of interest; the second step consisted in measuring the reaction time of finding these features for multiple values of their detection thresholds.

In this paper, we applied the proposed method to measuring saliency of stenoses placed at different geometrical locations along vessels. Experimental methods are described in section 2. Results are reported in section 3: measures of amplitude detection thresholds as a function of the mean 2-D curvature along the stenosis are given in section 3.1; reaction times for finding equally detectable stenoses at multiple values of the measured thresholds are reported in section 3.2. Results are discussed in section 4.

## 2. METHODS

In this paper, we focus on the detection of stenoses in 2-D angiograms. In angiograms, background complexity is two-fold: it is a function of the potential proximity of several blood vessels and also a function of the geometry of the blood vessels. The 2-D angiograms generated for the experiments use projections of 3-D vessels and the sum of their projections. Geometry of projected 3-D vessels can be quantified by the 2-D curvatures of the vessels in the projection plane. Proximity between blood vessels was controlled by spacing the vessels reasonably across the image and limiting the number of them to four or five. The number of grey pixels forming the vessels represented 16% of the image area,  $\pm 8\%$ . No stenosis was simulated near unusual locations such as extremely bright spots on the image, image boundaries, or where several vessels overlapped.

---

\* Image quality, here, is defined as how well desired information can be extracted from an image or a scene.

## 2.1 Stimuli

To generate a vessel, a 3-D space curve is specified within a 256 cubic pixel volume according to the Frenet formulas.<sup>23,17</sup> A 3-D vessel is then formed by rolling a solid sphere of desired diameter along the space curve. A stenosis is generated along a 3-D vessel by varying the diameter of the sphere. The diameter of the rolling sphere is described as a constant plus a Gaussian function centered at the location of the stenosis. The height and standard deviation of the Gaussian specify the degree of stenosis and the stenosis length, respectively. A 2-D vessel is then generated by projecting a 3-D vessel through the volume. An example of a projected 2-D space curve and the resulting 2-D vessel with a stenosis are shown in Figures 1a and 1b, respectively.

Three non-overlapping curvature categories were selected with mean values of 0.045, 0.135, and 0.20 and are referred to as medium, medium-high, and high curvatures. In a previous experiment, values of curvature in the order of 0.0085, referred to as low curvature, were also selected. Results from that experiment indicated no significant difference in median reaction times between low and medium curvatures and a significant difference between medium and high curvatures.<sup>1</sup> Thus, this experiment only involves medium, medium-high, and high curvatures. Images were 256 x 256 pixels, the diameter of the vessels and the length of the stenoses were constant and set to 12 and 20 pixels, respectively.

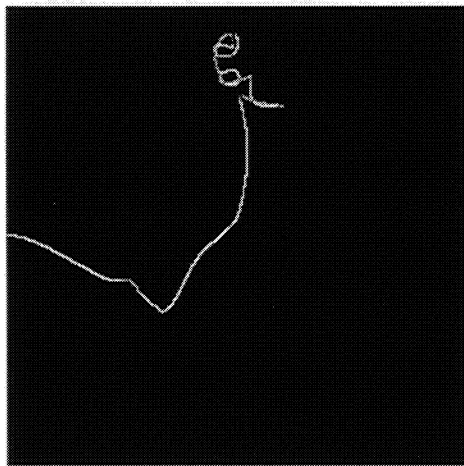


Figure 1a. *Projected 3-D space curve.*

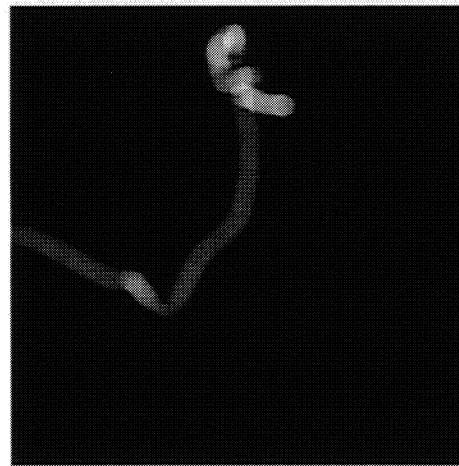


Figure 1b. *Projected 3-D blood vessel with a 50% stenosis .*

## 2.2 Subjects

Six subjects from 20 to 25 years old participated in experiment 1. All subjects had 20/20 or corrected vision and had no previous experience with reading angiograms. Three of these subjects participated in experiment 2: subjects 1, 2, and 3 reported in Table 1.

### 2.3 Experiment 1: measurement of stenosis amplitude detection thresholds

In this experiment amplitude detection thresholds of stenoses were measured at various geometrical locations. Measured thresholds and multiple values of the thresholds were then used to create appropriate stenoses amplitudes for the visual search experiment, referred to as experiment 2.

Stenoses amplitude detection thresholds were measured using a receiver operating curve (ROC) paradigm for eight vessels per curvature category.<sup>24-26</sup> Vessels with stenoses of varying amplitudes from 0% (no stenosis) to 26% were generated in increments of 2%. All vessels with all degrees of stenosis were presented within a block in random order. A total of thirty three blocks were presented, each with a different random order.

Images were displayed on a Sun SparcStation 10, using 128 greylevels. The display was photometrically linearized and the maximum brightness after linearization was 110 cd/m<sup>2</sup> for greylevel 127. Subjects sat in a dark room, approximately 0.5 m from the screen. Subjects were asked to rate their certainty of the presence of a stenosis on a continuous rating scale from 1 (absolutely not there) to 5 (certainly there).

Ratings for a vessel with a certain degree of stenosis were combined with those from the same vessel without a stenosis to compute an area under the ROC curve (AUC). An AUC was computed for each vessel and each degree of stenosis. The AUC was computed using the Wilcoxon algorithm that is based on a non-parametric estimation of the area.<sup>27</sup> For a given vessel, AUCs were then plotted as a function of the degree of stenosis, yielding a psychometric function.<sup>†</sup> The psychometric function was fit to a cumulative normal using PROBIT analysis. Stenosis amplitude detection threshold was defined as the percent stenosis corresponding to an AUC of 84%.

### 2.4 Experiment 2 : measurement of saliency

Visual search images were displayed on a non-interlaced Nanao 9080i RGB monitor with 256 greylevels and 120 Hz frame rate. Examples of stenoses at various curvature points are shown in Figure 2. The display was photometrically linearized with a maximum brightness of 143 cd/m<sup>2</sup>. One pixel covered 0.35 mm x 0.35 mm on the screen. Subjects sat in a dimly lit room, approximately 0.5 m from the screen. For each curvature category and subject, 100 images were generated at multiple values of the measured thresholds. Search time was typically recorded at 2, 4, 6, 8 and 10 times the thresholds. Subjects started with the highest value of the multiple value of the thresholds and ended with the lowest value. Before each session subjects run a block of 24 images to recall the task. After completion of the experiment, subjects rerun all conditions two to four days later, again starting with the highest value. This allowed us to investigate possible practice effects.

---

<sup>†</sup> The AUC in an ROC paradigm is equivalent to the percent correct in a 2 Alternative Force Choice (AFC) paradigm if the underlying probability density functions are Gaussian. Despite no such assumption is made here, it is from such an analogy that one can refer to a psychometric function when plotting AUC versus percent stenosis.

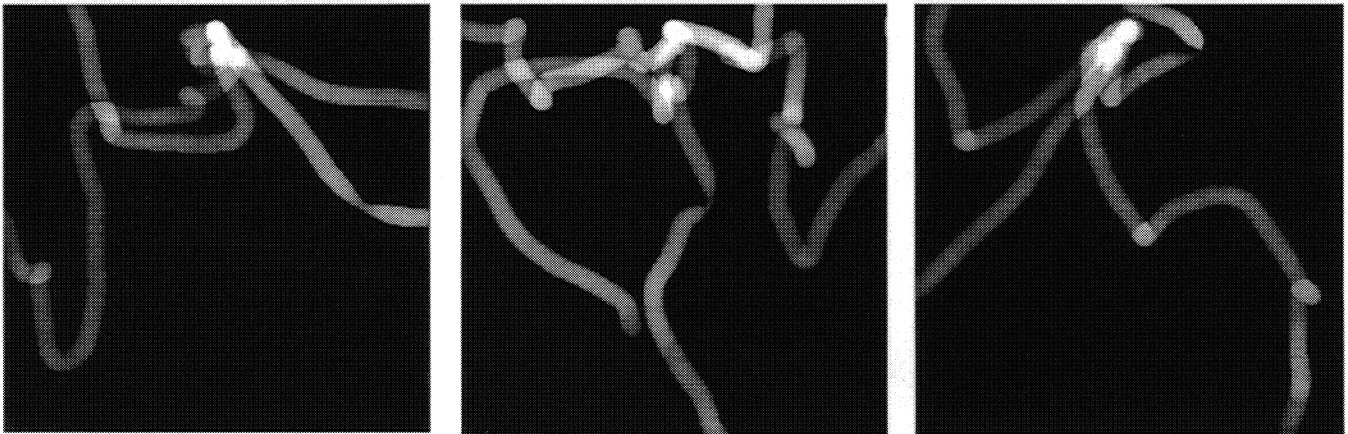


**Figure 2.** *Examples of stenoses at (a) medium, (b) medium-high, and (c) high 2-D mean curvature along vessels.*

The subject pressed a mouse button to start the experiment. In each trial, a single image was presented. All images contained a stenosis. When the stenosis was detected, the subject pressed one of three mouse buttons to signal whether the stenosis was detected in the left, middle, or right section of the display. At that time, the response time for detection was recorded unless the subject detected the stenosis in the wrong section of the display. The subject then used a trackball to specify the precise location of the stenosis within the selected section. By positioning a cursor with the trackball, the subject had to correctly identify the stenosis location within a circle of 20 pixels around the center of the stenosis or the trial was considered invalid. No time limit was imposed during localization of the detected stenosis. In 96 to 100 percent of the trials, stenoses were correctly localized for all three subjects. No feedback was provided to the subjects.

This procedure differs from traditional search methods, in which half of the images presented to the subjects contain a signal (in our case a stenosis) and half do not. One advantage of this procedure is the relatively low error rates and quasi-unbiased data compared to a traditional approach.<sup>28</sup>

## 3. RESULTS

### 3.1 Experiment 1

Stenosis amplitude detection thresholds for each subject are summarized in Table 1. Because of significant differences in subject sensitivity, thresholds for individual observers (1, 2, and 3) were used in experiment 2.

### 3.2 Experiment 2

Median reaction time was computed for each block of 100 trials in order to compute a robust estimate of performance. This approach is consistent with the results and recommendations of Ratcliff (1993).<sup>29</sup> One block corresponded to images with stenoses at one multiple value of the threshold and situated at one of three curvature categories.

in Figure 3, median reaction time is plotted versus multiple values of the measured thresholds (graphs on the left side) and versus percent stenosis (graphs on the right side) for each curvature category. Results for each subject are plotted separately. Subjects repeated the entire experiment twice to investigate potential practice effects. All results are summarized in Figure 3a-2l. Four consecutive plots correspond to the same subject (e.g. subject 1) and the extension to the subject number represents the run number (e.g. subject 1-2 for subject 1, run 2). The spreads of the distribution of responses around the median are represented as error bars corresponding to the values of the first quartile (25%) and the third quartile (75%). While these error bars were of the same order of magnitude for the first runs, they were only represented in the second runs for clarity.

subject #	Medium		Medium-high		High	
	MEAN	STDERR	MEAN	STDERR	MEAN	STDERR
1	10.1	0.6	10.6	0.5	13.3	0.6
2	8.4	0.4	11.1	0.8	11.8	1.2
3	9.6	0.7	12.6	0.7	20.9	3.3
4	12.7	0.5	13.8	0.7	28.7	3.4
5	28.3	0.6	34.4	1.4	44.3	2.8
6	12.0	0.5	16.9	0.8	22.6	1.9

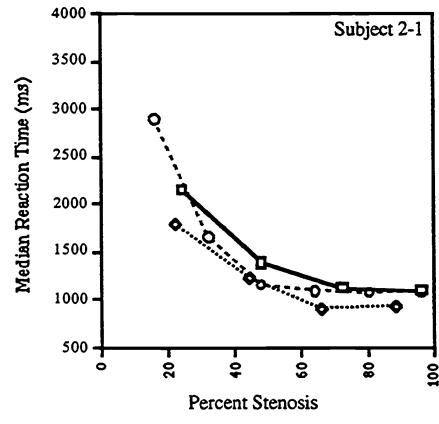
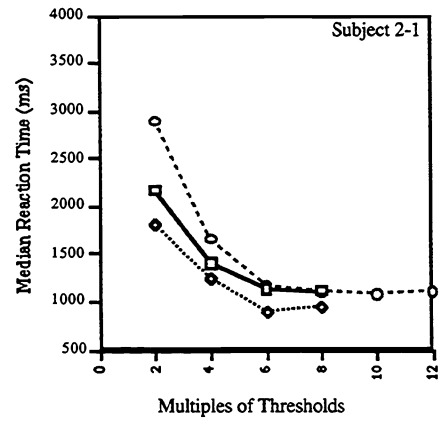
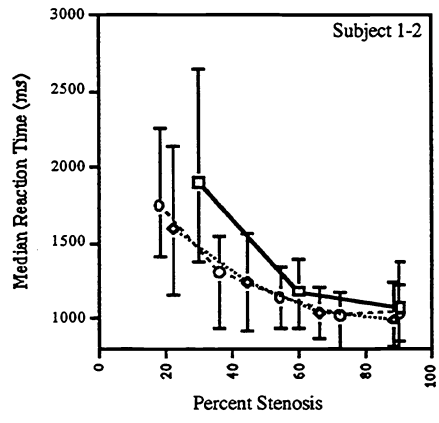
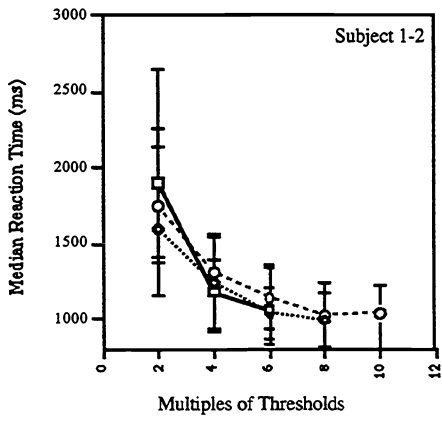
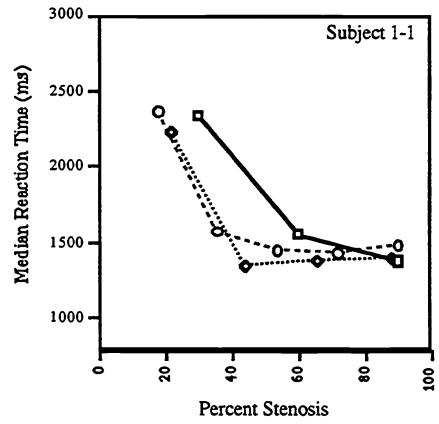
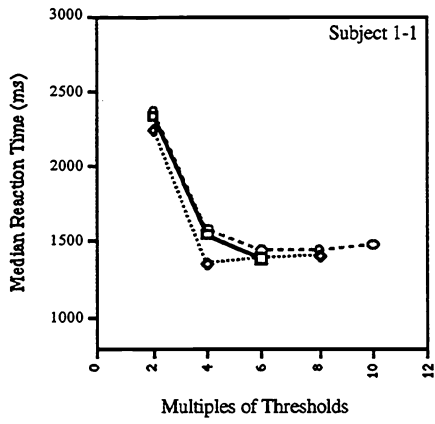
**Table 1.** Summary of stenosis amplitude detection thresholds for each subject: the mean corresponds to an average over eight blood vessels within a curvature category, and the stderr is the associated standard error.

## 4. DISCUSSION

In experiment 1, results indicate that stenosis amplitude detection thresholds increase for all three observers with curvature amplitudes.

In experiment 2, median reaction time plotted as a function of percent stenosis (graphs on the right, Figure 3) are higher for stenoses at high curvature points along a vessel, confirming our findings in a previous study.<sup>1</sup>

Median reaction time, plotted as a function of multiple values of thresholds, decreases monotonically for all curvatures and the three subjects. The curves flatten at stenoses amplitudes of about six times the measured thresholds for all three subjects. These amplitudes correspond to stenoses of 70 % to 95% for high curvatures, and 50% to 80% for medium-high and medium curvatures. Angiograms with stenoses below 75% are typically considered normal.<sup>30</sup> Therefore, results indicate that for clinically significant stenoses, geometry as measured here by the mean 2-D curvature along the stenosis does not impact saliency: all stenoses, once equalled in detectability in a location known-exactly task, are equally salient to a human eye.



- High
- ◆— Medium High
- Medium

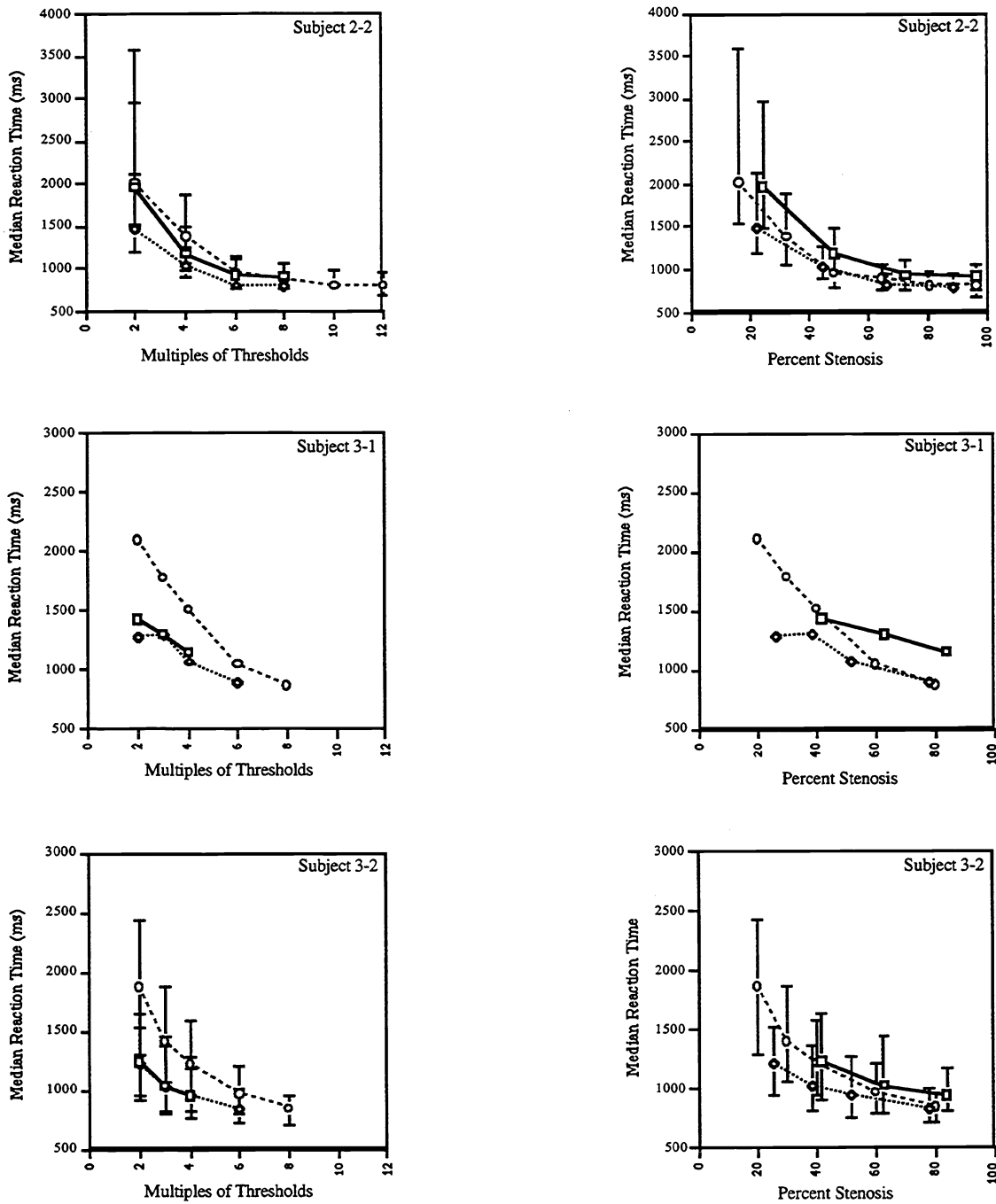


**Figure 3.** Median reaction time versus multiples of stenosis amplitude detection thresholds (left) and percent stenosis (right) for three subjects (1, 2, and 3). Results from two runs are reported. For a given subject (e.g. 2), the first two plots corresponds to the first run (e.g. Subject 2-1). The next two plots correspond to the second run (e.g. Subject 2-2). Error bars represent the first and third quartile of the distribution.

—□— High  
 .....◇..... Medium High  
 - - - ○ - - - Medium

Below a stenosis amplitude value of six times the measured thresholds, search times were independent of curvature for subjects 1 and 2. This is shown by the three overlapping curves in the plots “median reaction time” versus “multiples of thresholds” shown in Figure 3, subject 1-1 and 1-2. For subject 3, results show that search times were longer for stenoses at medium curvature than for stenoses at medium-high and high curvatures for stenosis amplitudes less than six times the thresholds or 80% stenosis. These results indicate that, for such amplitudes, stenoses at medium curvature were least salient for that subject. This finding is consistent across the two runs. It indicates that different search strategies may be involved for different subjects. Further investigations, however, remain to be done before definitive conclusions can be drawn. ‡

For all subjects, results also clearly indicate a practice effect shown by a downward shift of all the curves between run 1 and run 2. We are currently investigating performance at additional runs to quantify practice effects as well as to evaluate the robustness of the findings.

## 5. CONCLUSION

In a previous paper, we proposed a new methodology to measure object saliency in medical images, and more generally in complex natural backgrounds. Specifically, we proposed that relevant features be equalled in detectability in a location known-exactly task before saliency be measured in a visual search. In this paper, the methodology was applied to finding stenoses in angiograms. The independent variable was the 2-D mean curvature of the vessel along the stenosis. The dependent variable was the median reaction time to find a stenosis. Three subjects participated in the search study. Results indicate that for clinically significant stenoses (75% stenosis and higher), geometry as measured by the mean 2-D curvature along the stenosis does not impact saliency: all stenoses, once equalled in detectability in a location known-exactly task, are equally salient to the human eye.

## 6. ACKNOWLEDGMENTS

The authors would like to thank Stephen Pizer and Christina Burbeck for their stimulating discussions at an early stage of this research. We thank Paul Jaques for sharing his expertise with angiography. Many thanks go to Keith Muller and Deborah Glueck for their assistance with statistical analysis, Greg Abbey for providing us with the implementation of the Delong-Delong algorithm used to analyse the thresholds data, Ben Tsui for providing software for ROC data collection, and Arthur Burgess for stimulating discussions about the interpretation of the data. Finally, we thank our human subjects for their kind participation. This research was supported by NIH PO-CA47982.

---

‡ It must be noted that subject 3, whose performance favored higher curvature locations in the search experiment, did not fully comply with the protocol used in measuring the stenoses amplitude thresholds. This observer used the rating scale in a non-continuous fashion, essentially using the two extremes of the scale. However, because the data were found to be consistent and reliable, we chose to include that subject in the visual search experiment.

## 7. REFERENCES

1. J.P. Rolland, K. Muller, and C.S. Helvig, "Visual search in medical images : a new methodology to quantify saliency," *Medical Imaging 1995*, Proc. Of the SPIE 2436, 1995.
2. R.G. Swensson, S.J. Hessel, and P.G. Herman, "Omissions in radiology: faulty search or stringent reporting criteria," *Radiology*, 123 (3), pp. 563-567, 1977.
3. L. W. Nolte, and D. Jaarsma, "More on the detection of one of M orthogonal signals," *Journal of the Acoustical Society of America*, 41, pp. 497-505, 1967.
4. S.J. Starr, C.E. Metz, L.B. Lusted, and D.J. Goodenough, "Visual detection and localization of radiographic images," *Radiology* 116, pp. 553-538, 1975.
5. A.E. Burgess, and H. Ghandeharian, "Visual signal detection. II. signal-location identification," *J. Opt. Soc. Am. A*, 1, pp. 906-910, 1984.
6. Pelli, D.G., "Uncertainty explains many aspects of visual contract detection and discrimination," *J. Opt. Soc. Am. A*, 2, pp. 1508-1532, 1985.
7. R.G. Swensson, "Measuring detection and localization performance," *Information Processing in Medical Imaging*, H.H. Barrett and A.F. Gmitro, Springer-Verlag, pp. 525-541, 1993.
8. K.J. Myers, J.P. Rolland, H.H. Barrett, and R.F. Wagner, "Aperture optimization for emission imaging: effect of a spatially varying background," *J. Opt. Soc. Am. A*, 7, pp. 1279-1293, 1990.
9. J.P. Rolland and H.H. Barrett, "Effect of random background inhomogeneity on observer detection performance," *J. Opt. Soc. Am. A*, 9, pp. 649-658, 1992.
10. H.H. Barrett, J. Yao, J. P. Rolland, and K. J. Myers, "Model observers for assessment of image quality," *Proc. Natl. Acad. Sci.* 90, pp. 9758-9765, 1993.
11. A.E. Burgess, and X.li, "experimental evaluation of observer models for detection of signals in statistically defined backgrounds," *Information Processing in Medical Imaging*, Y. Bizais et al., Kluwer Academic Publishers, pp. 89-100, 1995.
12. J. Yao, and H.H. Barrett, "Predicting human performance by a channelized Hotelling observer model," *Proc. of the SPIE* 1768, pp.161-168, 1992.
13. P.F. Judy, "Detection of clusters of simulated calcifications on lumpy noise backgrounds," *Proc. of the SPIE* 2712, 1996.
14. H.L. Kundel, C.F. Nodine, and E.A. Krupinski, "Searching for lung nodules: visual dwell indicates locations of false-positive and flase negative decisions," *Investigative Radiology* 24(6), pp. 472-478, 1989.
15. E.A. Krupinski, C.F. Nodine, and H.L. Kundel, "perceptual enhancement of tumor targets in chest X-ray images," *Perception and Psychophysics* 53(5), pp.519-526, 1993.
16. G. Revesz, H.L. Kundel, and M.A. Graber, "The influence of structured noise on detection of radiologic abnormalities," *Invest. Radiol.* 9, pp. 479-486, 1974.
17. J.P. Rolland, and D.T. Puff, "Angiogram simulation software documentation," *University of North Carolina Department of Computer Science, Technical Report TR93-018*, 1993.
18. T. Sandor, and R.G. Swensson, "Evaluation of observer performance in detecting blood vessels on simulated angiographic images," *Med. Phys.* 5(5), pp. 380-386, 1978.
19. J. Tobis, O. Nalcioğlu, L. Iseeri, et al., "Detection and quantitation of coronary artery stenoses from digital subtraction angiograms compared with 35 millimeter film cineangiograms," *Am. J. Cardiol* 54, pp. 489-496, 1984.

20. P. Jaques, F. DiBianca, S. Pizer, F. Kohout, L. Lifshitz, and D. Delany, "Quantitative digital fluorography: computer vs. human estimation of vascular stenoses," *Investigative Radiology*, 20, pp. 45-52, 1985.
21. J. Ambrose, S.L. Winters, A. Stern, A. Eng, L.E. Teichholz, R. Gorlin, and V. Fuster, "Angiographic morphology and the pathogenesis of unstable angina pectoris," *J. Am. Coll. Cardiol.* 5(3), pp. 609-616, 1985.
22. J. Palmer, "Visual search latency: the influence of target distractor discriminability on the magnitude of set-size effects," *Investigative Ophthalmology and Visual Science*, 35(4), (abstract), 1994.
23. O'Neill, Barrett. *Elementary Differential Geometry*. Orlando: Academic Press, 1966.
24. J.P. Egan, *Signal Detection Theory and ROC Analysis*, Academic Press, NY, 1975.
25. C.E. Metz, "ROC methodology in radiologic imaging," *Invest. Radiol.* 21, pp.720-733. 1986.
26. J.A. Swets, "Measuring the accuracy of diagnosis systems," *Science* 240, pp. 1285-1293, 1988.
27. E.R. DeLong, D.M. DeLong, and D.L. Clarke-Pearson, "Comparing the areas under two or more correlated receiver operating characteristic curves: a nonparametric approach," *Biometrics* 1988, 44, pp. 837-845, 1988.
28. J. Elder, and S. Zucker, "The effect of contour closure on the rapid discrimination of two-dimensional shapes," *Vision Research*, 33(7), pp 981-991, 1993.
29. R. Ratcliff, "Methods for dealing with reaction time outliers," *Psychophysical Bulletin*, 114 (3), pp. 510-532, 1993.
30. T.B. Kinney, and S.C. Rose, "intraarterial pressure measurements during angiographic evaluation of peripheral vascular disease: techniques, interpretation, applications, and limitations," *AJR* 166, pp. 277-284, 1996.